JOURNAL OF APPLIED ELECTROCHEMISTRY **25** (1995) 1105–1112

Application of metallic foams in an electrochemical pulsed flow reactor
Part I: Mass transfer performance

P. COGNET*, J. BERLAN*, G. LACOSTE‡

**Laboratoire de Synthèse Organique en Milieux Polyphasiques and ‡Laboratoire de Génie Electrochimique et d'Energétique des Réacteurs, Ecole Nationale Supérieure d'Ingénieurs de Génie Chimique, 18 chemin de la Loge, 31078 Toulouse, Cedex, France*

P.-L. FABRE

Laboratoire de Chimie Inorganique, EA 807, Université Paul Sabatier, 118 route de Narbonne, 31062 Toulouse, Cedex, France

J.-M. JUD

E.D.F./D.E.R., Les Renardières, B.P. no. 1, 77250 Moret sur Loing, France

Received 10 June 1994; revised 20 February 1995

This paper describes mass transfer in a porous percolated pulsated electrochemical reactor (E3P reactor), fitted with nickel foam electrodes in an axial configuration.The work is aimed at optimization of the mass transfer conditions in electroorganic reactions such as the oxidative cleavage of diols or the conversion of DAS (diacetone-L-sorbose) into DAG (diacetone-2-keto-L-gulonic acid). The use of nickel foam as an electrode material is of interest for these electrocatalytic reactions due to its high specific surface area (4000 to 11 000 m^{-1}) and its high porosity (over 0.97). The electroreduction of ferricyanide has been chosen as a test reaction in order to correlate the mass transfer coefficient with the overall flow velocity and the amplitude and frequency of the electrolyte pulsation. Four foam grades have been tested.

List of symbols

a	pulsation amplitude (m)
A_{ve}	dynamic specific area of the foam: surface area per volume of material (m^{-1})
C	ferricyanide concentration in the cell ($mol\,m^{-3}$)
D	diffusion coefficient of ferricyanide ($m^2\,s^{-1}$)
d_m	mean path of a particle in the three-dimensional electrode (m)
d_R	diameter of the reactor column (m)
d_p	mean foam pore diameter of the foam (m)
e	thickness of the electrode bed (m)
f	pulsation frequency (Hz)
F	Faraday number ($C\,mol^{-1}$)
I	limiting diffusion current (A)
k_d	mass transfer coefficient with pulsation ($m\,s^{-1}$)
k_0	mass transfer coefficient without pulsation ($m\,s^{-1}$)
n	number of electrons in the electrochemical reaction
Q_V	volummetric flow rate through the reactor ($m^3\,s^{-1}$)
Re	Reynolds number $Re = U_0 d_R \nu^{-1}$
Re_{pore}	Reynolds number based on mean pore diameter d_p, $Re_{pore} = \rho U_0 \tau d_p \epsilon^{-1} \mu^{-1}$
S	active surface area of the electrode (m^2)
Sc	Schmidt number, $Sc = \nu D^{-1}$
Sh	Sherwood number, $Sh = k_d d_R D^{-1}$
Sh_{pore}	Sherwood number based on mean pore diameter d_p, $Sh_{pore} = k_d d_p D^{-1}$
Sr	Strouhal number, $Sr = a\omega U_0^{-1}$
t_r	mean residence time (s)
U_0	permanent superficial velocity, $U_0 = Q_v/(\pi d_R^2/4)$ ($m\,s^{-1}$)

Greek letters

ϵ	porosity of the foam
μ	dynamic viscosity ($kg\,m^{-1}\,s^{-1}$)
ν	kinematic viscosity ($m^2\,s^{-1}$)
ρ	liquid density ($kg\,m^{-3}$)
ω	pulsation, $\omega = 2\pi f$ ($rad\,s^{-1}$)
τ	tortuosity of porous medium

0021-891X

1. Introduction

The E3P (porous percolated pulsed electrode) reactor is characterized by pulsation of the liquid phase through a porous electrode [1, 2]. This reactor represents a good compromise between a fixed electrode, which can be easily blocked, and a fluidized electrode which exhibits low conductivity. It was first applied to the treatment of waste effluents and recovery or dissolution of metals [3–5]. Later, it was applied to different electrochemical processes such as the electrosynthesis of polypyrrole [6, 7] or the electrodeposition of a poly(dibenzo-18-crown-6) film [8, 9]. Recently, it has been shown to be of interest in organic electrosynthesis [10]. Both amplitude and frequency of the pulsation appear to be key parameters. In two phase systems, pulsation enhances emulsion stability. Moreover, the mass transfer conditions and selectivity are enhanced.

To continue these studies, an investigation of the electrooxidation of diols with the E3P on nickel foam electrodes was carried out. Electrodes of high specific surface areas are of great interest for these electrocatalytic oxidation processes [11–13]. They are generally used in alkaline media with very low current densities. However, high currents processes have also been described [14].

Interesting properties of nickel foam have been outlined in previous papers, concerning its structure [15, 16, 17] and its application as a three-dimensional electrode in various electrochemical reactors [18, 19]. More precisely, hydrodynamics [19], experimental electrode potential distributions [20, 21], axial dispersion in a liquid flow [22] and mass transfer [23, 24] were studied.

In this paper we report the mass transfer performance of the reaction at a nickel foam electrode. An axial configuration in an undivided cell was chosen. Mass transfer determinations were carried out with the ferro–ferricyanide electrochemical system.

2. Experimental details

Experiments were carried out in an E3P reactor as shown in Fig. 1 (the internal volume was $10^{-3}\,m^3$) [25]. A peristaltic pump (2) was used to control the permanent superficial velocity, U_0. Pulsation was achieved by means of a Teflon piston (with $0 < a < 0.014\,m$ and $0 < f < 1.24\,Hz$). The instantaneous velocity of the liquid is given by

$$U = U_0 + a\omega \sin \omega t \qquad (1)$$

and the hydrodynamic conditions can be characterized by the Strouhal number $Sr = a\omega/U_0$ [2]. In the present study, as $Sr \gg 1$, the electrochemical cell can be considered as a perfect stirred tank, to a first approximation [1].

Circular sheets of four grades of nickel foam from Sorapec, Paris [26] were used as electrodes. Their characteristics are listed in Table 1. The porosity of these foams is in the 0.97–0.98 range [17] and the

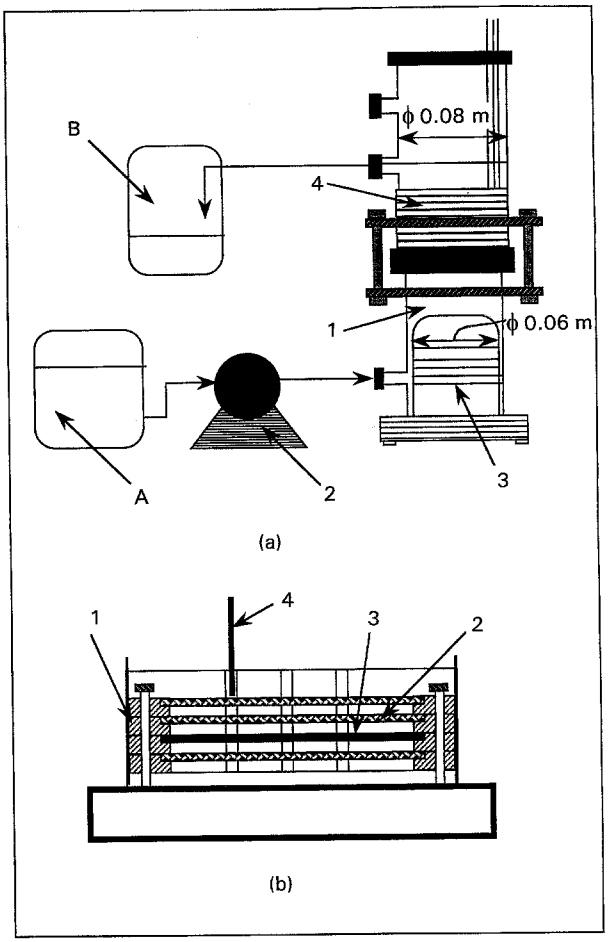

Fig. 1. Schematic view of the E3P reactor: (a) 1 reactor, 2 pump, 3 piston, 4 electrodes: (b) electrodes stand, 1 Teflon frame, 2 auxiliary electrode, 3 nickel foam working electrode, 4 ECS reference electrode.

electrode surface area lies in the range 0.04–0.1 m^2. Only one nickel electrode was connected; the other electrodes were used as turbulence promoters. The auxiliary electrode was made of nickel plated expanded copper (area 0.14 m^2).

Experiments were carried out as follows: (i) the electrodes were cleaned *in situ* with a 0.05 M sulfuric acid solution; (ii) the working electrode was cathodically activated in a 0.5 M KOH solution (2 A for 0.5 h); and (iii) the electrolyte (a mixture of 0.01 M $K_3Fe(CN)_6$ and 0.1 M $K_4Fe(CN)_6$ in 0.5 M KOH), was pumped from storage tank A (at 25 °C), to the lower part of the reactor and collected in tank B (Fig. 1(a)). It was not recycled in order that the ferricyanide concentration at the working electrode might remain constant. The physical properties of the mixture are given in Table 2.

Table 1. Physical properties of nickel foams

Grade	*Number /pores per linear inch*	*Mean pore diameter, d_p/mm*	*Thickness* /mm	A_{ve} /m^{-1}
MN 020	20	1.8	5	1800
MN 045	45	0.45	2	4000
MN 060	60	0.3	2	5500
MN 100	100	0.2	1.7	9000

Table 2. Physical properties of the solution at 25 °C

Property	*Value*
Kinematic viscosity, ν	$1 \times 10^{-6}\,m^2\,s^{-1}$
Density, ρ	$1020\,kg\,m^{-3}$
Diffusion coefficient of ferricyanide, D	$104 \times 10^{-10}\,m^2\,s^{-1}$
Schmidt number Sc	990

Under potentiostatic conditions with a three electrode configuration, the working electrode potential was set to −0.3 V vs SCE, where the reduction of $K_3Fe(CN)_6$ was under diffusion control, while the oxidation of $K_2Fe(CN)_6$ occurred at the counter electrode. The overall cell potential (electrochemical potential plus ohmic drop) was lower than 2 V and no dioxygen evolution was observed.

The mass transfer study was carried out with 190 experimental points for each foam grade in order to obtain the correlations (Tables 4 to 6). The parameters of the correlations, listed in Table 4, were calculated by using six values of a and five values of ω.

3. Results and discussion

3.1. *Reactor characterization*

Pulsation of the solvent in the E3P reactor was carried out at high Strouhal number which means that the flow was periodically reversed. Due to this push–pull displacement, the electroactive species cross the electrode bed several times. Moreover, the mass transfer is modified by the instantaneous electrolyte velocity which controls the diffusion layer thickness.

Figure 2 represents the vertical displacement of a particle in the reactor. In the three-dimensional electrode, it is observed that the mean path d_m of the particle is higher under pulsation than without pulsation ($d_m = e$). Since the residence time is equal to e/U_0, a higher value of d_m implies higher mass transfer coefficient. Thus, the measurement of d_m is important to the study of mass transfer. The determination of d_m is obtained by the calculation of the particle displacement in the three-dimensional electrode (vertical arrows in Fig. 2). At $t = 0$, the particle is at the edge of the three-dimensional electrode of thickness e. Subsequently, its vertical position $z(t)$ is related to the linear velocity, U_0, and the pulsation parameter:

$$z(t) = U_0 t + a\cos(\omega t) - a$$

The particle enters the three-dimensional electrode several times from cycle 0 to cycle $n_s - 1$. The mean path of the particle is the sum of the vertical $z(t)$ variation (Fig. 2) and is expressed by [27]

$$d_m = \sum_{i=1}^{n_e-1} 2z_{h,i} - \sum_{i=n_0}^{n_s-1} 2z_{b,i} + e + 2(n_s - n_e)e$$

where $z_{h,i}$ is the vertical position for $t = 2\pi i$, corresponding to the maxima of the curve, is given by

$$z_{h,i} = z(2\pi i) = \frac{U_0 i}{f}$$

and $z_{b,i}$ is the vertical position for $t = 2\pi i + \pi$, corresponding to the minima of the curve, is given by

$$z_{b,i} = z(2\pi i + \pi) = \frac{U_0(2n+1)}{2f} - 2a$$

n_0 is the number of periods when z_{b,n_0} is in the three-dimensional electrode and is defined by an integer:

$$\frac{U_0(2n_0+1)}{2f} - 2a > 0 \text{ that is } n_0 > \frac{2af}{U_0} - 0.5$$

n_e is the number of periods when z_{h,n_e} is above the three-dimensional electrode and is defined by an integer:

$$\frac{U_0 n_e}{f} > e, \quad \text{that is, } n_e > \frac{ef}{U_0}$$

n_s is the number of periods when z_{b,n_s} is above the three-dimensional electrode (the particle leaves definitively the electrode bed) and is defined by an integer:

$$\frac{U_0(2n_s+1)}{2f} - 2a > e$$

that is

$$n_s > \frac{ef}{U_0} + \frac{2af}{U_0} - 0.5$$

Taking into account the values of $z_{h,i}$ and $z_{b,i}$, d_m is expressed as

$$d_m = \frac{2U_0}{f}\sum_{i=1}^{n_e-1} i + 4a(n_s - n_0) - \frac{U_0}{f}\sum_{i=n_0}^{n_s-1}(2i+1) + e(2n_s - 2n_e + 1)$$

and the final result is

$$d_m = e(2n_s - 2n_e + 1) + 4a(n_s - n_0) + \frac{U_0}{f}(n_e^2 + n_0^2 - n_s^2 - n_e + 1)$$

It must be pointed out that the residence time is unchanged whatever the pulsation and depends only

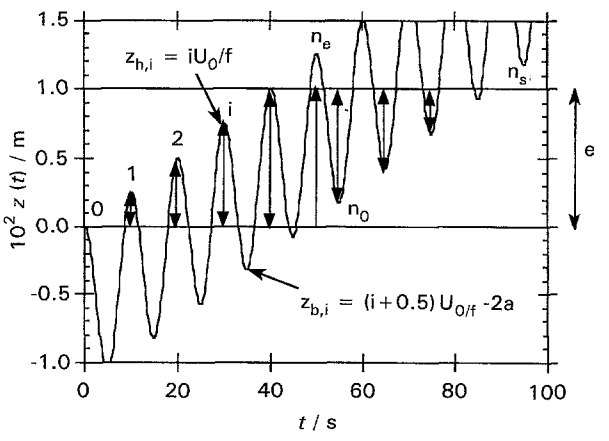

Fig. 2. Schematic diagram of the vertical position for a particle in the volumic electrode of the E3P reactor: $a = 6 \times 10^{-3}$ m; $f = 0.1$ Hz; $U_0 = 2.5 \times 10^{-4}\,m\,s^{-1}$.

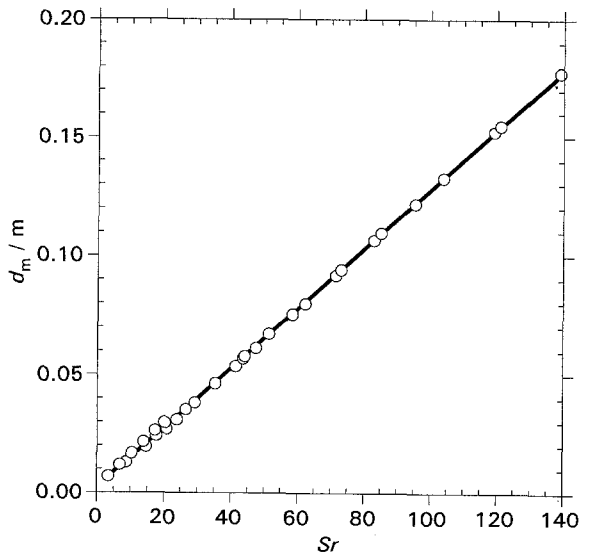

Fig. 3. Variation of the mean course d_m with Sr for a nickel foam electrode of thickness 2 mm as a function of Strouhal number Sr.

on the linear velocity $t_r = e/U_0$. Fig. 3 represents the mean course, d_m, of a particle in a three-dimensional electrode of thickness 2 mm as a function of Strouhal number Sr. The conditions are those of a nickel foam electrode MN100 which was used in the mass transfer study. A linear correlation appears between the mean course, d_m, and Strouhal number, Sr, used in the present study. For $Sr = 0$ (no pulsation) d_m is evidently equal to e. The linearity between d_m and Sr is explained by the equation of d_m in which appear n_s and n_0, n_s and n_0 being related to the ratio $2af/U_0$, i.e. to Sr/π. As in our experiments ef/U_0 is lower than $2af/U_0$, the mean course d_m is effectively controlled by the Strouhal number Sr. As shown in Fig. 3, the mean course d_m can be increased from 2 mm with no pulsation up to nearly 200 mm for a Strouhal number of 140. If d_m is increased while the residence time t_r is constant, the mean electrolyte velocity d_m/t_r in the three-dimensional electrode is increased in the same manner. This average electrolyte velocity controls the average diffusion layer thickness and, consequently, the mass transfer coefficient at the electrode. That means that the mass transfer must be higher under pulsation and will depend on the Sr number.

3.2. *Mass transfer study*

The mass transfer coefficient between the liquid and the electrode was obtained by means of the cathodic reduction of ferricyanide ions. The limiting current, I, was measured as a function of the superficial velocity, U_0, the amplitude, a, and the frequency, f, of the pulsation. This study was made with and without pulsation. In the first case, the average pulsating intensity was taken into account.

The permanent electrolyte superficial velocity, U_0, was varied between 4 and 30×10^{-4} m s^{-1}. The Strouhal number Sr was varied from 4 to 300. The Reynolds number based on reactor diameter, d_R, was in a 30 to 250 range. In the reactive zone, a Reynolds number was calculated from the liquid density ρ, the dynamic viscosity μ, the mean pore diameter d_p and the mean velocity v $(=U_0\tau\epsilon^{-1})$ in the pores [22]: $Re_{pore} = v\rho d_p \mu^{-1}$. This particular Reynolds number, characteristic of the hydrodynamic conditions inside the three-dimensional electrode for each foam, is useful in the calculation of general correlations between Sh_{pore} and Re_{pore}.

Table 3. Experimental variations of k_0 against U_0 without pulsation

Grade of foam	*Correlated k_0 against U_0*
MN020	$k_0 = 3.33 \times 10^{-5} \times U_0^{0.28}$
MN045	$k_0 = 2.62 \times 10^{-5} \times U_0^{0.25}$
MN060	$k_0 = 5.38 \times 10^{-5} \times U_0^{0.36}$
MN100	$k_0 = 15.80 \times 10^{-5} \times U_0^{0.42}$

3.2.1. Mass transfer coefficient at the nickel foam electrode. The electrode is three-dimensional. The dynamic specific areas, A_{ve}, of the four grades of foam are given by the supplier [26]. They are of the same magnitude as those measured by permeametry by Montillet [17]. These values will be used in the following calculations as the effective mass transfer surface areas of the foams.

As the potential is on the plateau of the reduction wave of $K_3Fe(CN)_6$, the mass transfer coefficient, k_d, is calculated from Equation 2:

$$k_d = \frac{I}{nFcS} = \frac{1.04\,I}{S} \qquad (2)$$

assuming a constant value of the bulk concentration C. The conversion of ferricyanide for each complete passage of the electrolyte was found to be negligible.

Without pulsation, the mass transfer coefficient is k_0 and is related to the velocity U_0 according to the foam grade (Table 3). Under pulsation, the mass transfer coefficient is related to the velocity U_0 and the pulsation parameters (Table 4).

Taking into account the correlated values of k_d, Correlations 3 and 4 were obtained from mass transfer data with four nickel foam electrodes of different grade:

$$Sh = \alpha\, Sc^{1/3} Re^{\beta} \quad \text{(without pulsation)} \qquad (3)$$

$$Sh = \alpha\, Sc^{1/3} Re^{\beta} Sr^{\gamma} \quad \text{(with pulsation)} \qquad (4)$$

The values of α, β and γ are given in Table 5.

3.2.2. Mass transfer at a nickel foam sheet without pulsation. The experimental values of k_0 for different

Table 4. Experimental variations of k_d against U_0, ω and a under pulsation

Grade of foam	*Correlation K_d against U_0, a, ω*
MN020	$k_d = 4 \times 10^{-5} \times U_0^{0.0} \times a^{0.39} \times \omega^{0.39}$
MN045	$k_d = 4 \times 10^{-5} \times U_0^{0.01} \times a^{0.27} \times \omega^{0.27}$
MN060	$k_d = 16.7 \times 10^{-5} \times U_0^{0.22} \times a^{0.32} \times \omega^{0.32}$
MN100	$k_d = 8.5 \times 10^{-5} \times U_0^{0.01} \times a^{0.41} \times \omega^{0.41}$

Table 5. Correlation coefficients expressed as Sh against Re and Sr without and under pulsation: 30 < Re < 250 and 4 < Sr < 300

Grade of foam	$Sh = \alpha Sc^{-1/3} Re^{\beta}$ *(without pulsation)*	$Sh = \alpha Sc^{-1/3} Re^{\beta} Sr^{\gamma}$ *(under pulsation)*
MN020	$\alpha = 10.8$ $\beta = 0.28$	$\alpha = 3.7$ $\beta = 0.39$ $\gamma = 0.39$
MN045	$\alpha = 12.0$ $\beta = 0.25$	$\alpha = 6.6$ $\beta = 0.34$ $\gamma = 0.27$
MN060	$\alpha = 7.1$ $\beta = 0.36$	$\alpha = 2.8$ $\beta = 0.54$ $\gamma = 0.32$
MN100	$\alpha = 10.5$ $\beta = 0.42$	$\alpha = 5.5$ $\beta = 0.42$ $\gamma = 0.41$

U_0, without pulsation, are given in Table 3 and plotted in Fig. 4. As shown in Fig. 4, a linear correlation appears between $\log(k_0)$ and $\log(U_0)$.

Except for the grade MN020, the coefficient of *Re* increases from 0.25 to 0.42 together with the specific surface area of the foam. Foams with the smallest pore diameters are more sensitive to the permanent superficial velocity. The best mass transfer coefficients are obtained with the MN100 foam. They are twice as large as those obtained with foams MN020, MN045, MN060, under the same hydrodynamic conditions. The latter give coefficients of the same magnitude. A general correlation for each grade of foam was thus determined:

$$Sh_{\text{pore}} = Re_{\text{pore}} Sc^{1/3} - 16.90\, d_p/d_r\, Re^{\beta} Sc^{1/3} \quad (5)$$

in which β depends on the foam grade.

3.2.3. Mass transfer at a nickel foam sheet under pulsation. The results obtained with pulsation are given in Table 4. The influence of both amplitude and frequency of pulsation on the mass transfer is almost the same: the exponents of a and ω in the expressions given in Table 4 are the same. The variations of k_d with ω are shown in Fig. 5. k_d increases with ω but seems to reach a limit that could not be observed owing to the limits of the reactor performance. Frequency and amplitude of pulsation dramatically increase mass transfer.

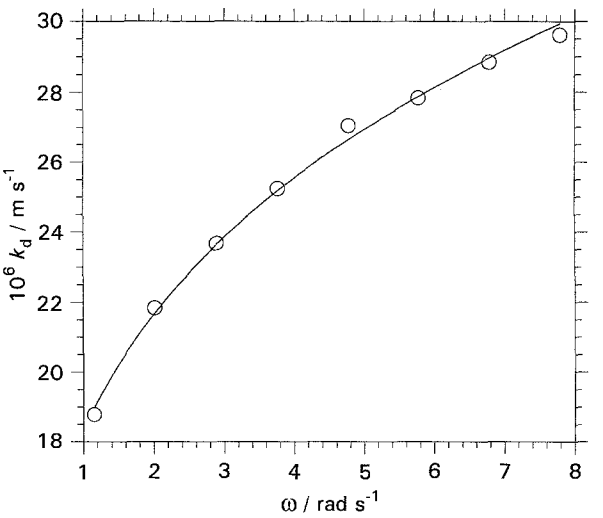

Fig. 5. Variation of the mass transfer coefficient k_d with frequency ω for a MN100 foam electrode: $U_0 = 23.4 \times 10^{-4}$ m s^{-1}; $a = 0.014$ m.

Taking into account the correlations of Table 4, Fig. 6 shows the linearity between $\ln(k_d)$ and $\ln(Sr)$. Among the different foam grades, MN100 appears to be the more efficient in terms of mass transfer: k_d can reach 2×10^{-5} m s^{-1}. Unexpectedly, MN020 behaves in a different manner from the other grades. This behaviour cannot be explained at present.

Fig. 7 shows the variations of the mass transfer coefficient as a function of the mean path, d_m, in the nickel foam electrode MN100 for different values of

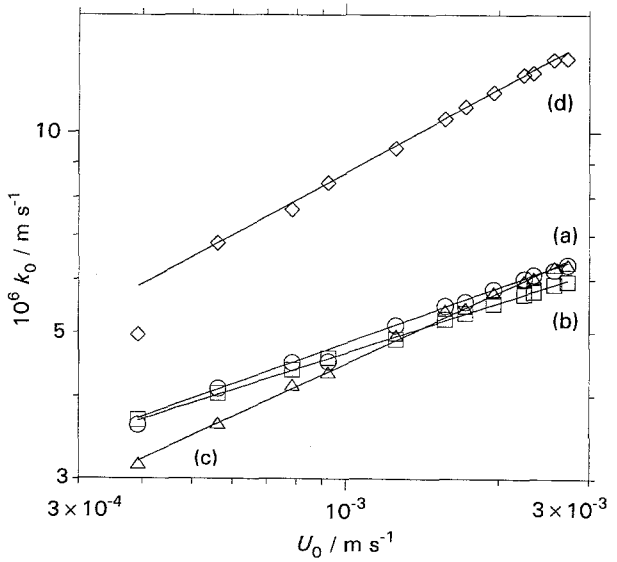

Fig. 4. Experimental data and correlations expressed by K_0 against U_0, without pulsation: (a) MN020 foam, (b) MN045 foam, (c) MN060 foam, (d) MN100 foam.

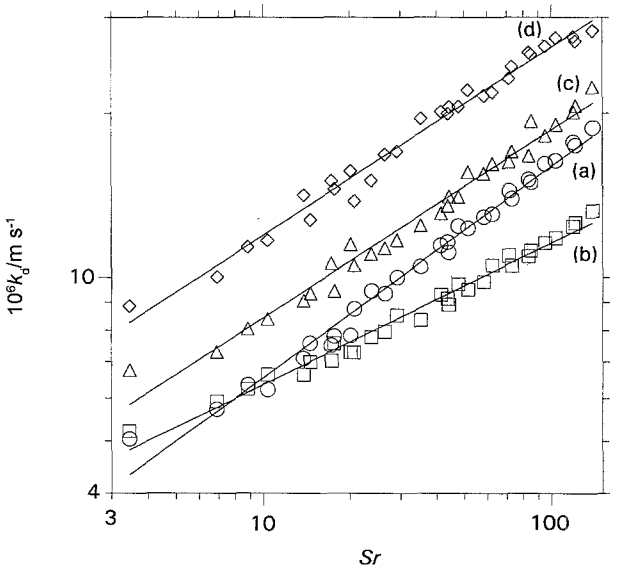

Fig. 6. Variations of the mass transfer coefficient k_d with Strouhal number Sr for a fixed velocity, $U_0 = 7.8 \times 10^{-4}$ m s^{-1}: (a) MN020 foam, (b) MN045 foam, (c) MN060 foam, (d) MN100 foam.

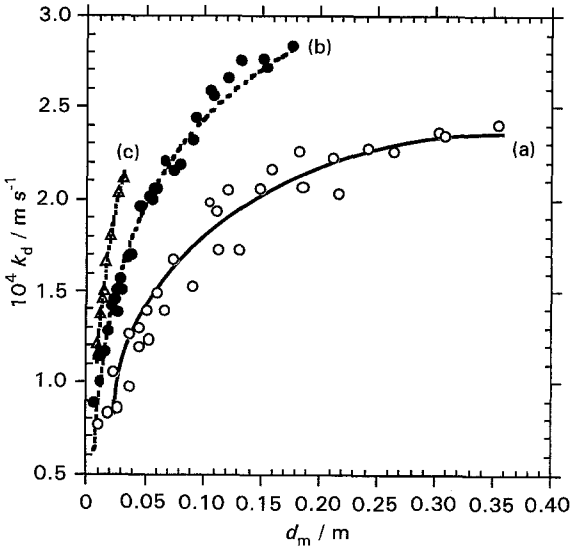

Fig. 7. Variations of the mass transfer coefficient k_d with the mean course d_m for a nickel foam electrode MN100. Permanent velocity, U_0: (a) 3.9×10^{-4}, (b) 7.8×10^{-4} and (c) 15.7×10^{-4} m s^{-1}.

U_0. The same shape as in Fig. 5 can be observed, which is normal since d_m is a linear function of Sr. Effectively, correlation factors of k_d as a function of d_m have the same order of magnitude as those obtained for k_d as a function of ω (Table 4).

At low U_0, the variation of k_d with d_m seems to be logarithmic: k_d is limited at high d_m when under high pulsation.

It is observed that, except for the MN020 foam, the exponent of $(a\omega)$ is of the same order of magnitude as the exponent of U_0 in the correlation without pulsation. According to Equation 1, transfer mainly depends on pulsation, since $a\omega$ becomes the major factor. This is confirmed by the trend of k_d/k_0 [10], which is greater for low superficial velocities: pulsation is more efficient with low flow rates, as shown in Fig. 8.

Earlier studies were carried out with the same type of reactor [10]. The study of electrochemical reduction

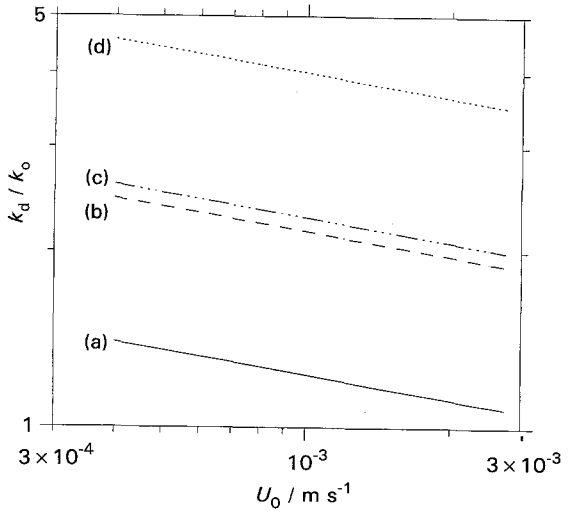

Fig. 8. Correlations expressed by k_d/k_0 against U_0 for different pulsation parameters, a (m), f (Hz), at a nickel foam electrode MN60: (a) (0.0024, 0.18), (b) (0.014, 0.18), (c) (0.0024, 1.24), (d) (0.0140, 1.24).

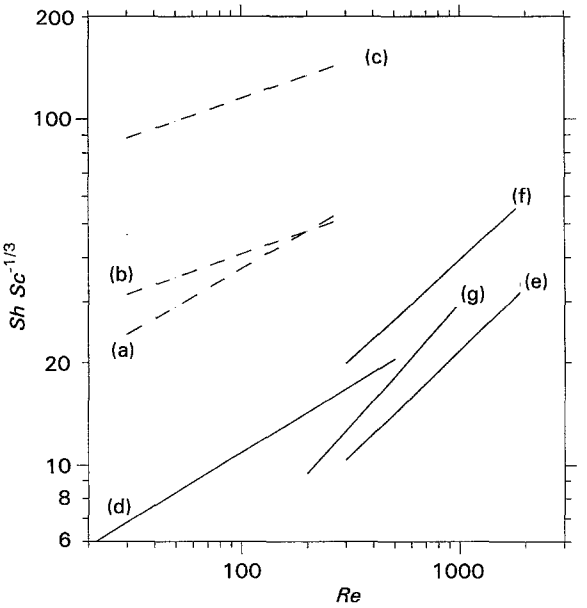

Fig. 9. Correlations expressed by $Sh\ Sc^{1/3}$ against the Reynolds number Re for different electrode configuration: (a, b, c) present work a nickel foam electrode MN060; (a) without pulsation, (b, c) under pulsation parameters a (m), f (Hz) with (b) = (0.002, 0.2) and (c) = (0.01, 1) (d–g) mass transfer in a filter-press reactor with (d) nickel sheet of foam G60 p.p.i. [23], (e) nickel plate of foam G60 p.p.i. [24], (f) plane plate with a turbulence promoter [24], (g) plate alone [28].

of acetophenone at a cadmium electrode gave the following correlation: $k_d/k_0 = 12.19\ a^{0.38}\omega^{0.37}$. The coefficients of a and ω are identical and the coefficients are of the same order of magnitude. The amplitude and frequency of the pulsation have the same effect on mass transfer at a plane electrode in an axial configuration. The performance of the E3P reactor is similar whatever the electrochemical process.

E3P reactor performances can be compared to those of filter-press reactors [24]. Correlations are expressed as

$$Sh = \alpha\, Sc^{-1/3} Re^{\beta} Sr^{\gamma}$$

Results are gathered in Table 6. The correlations for the MN060 foam are plotted in Fig. 9 for comparison with results for the same foam in a filter-press cell. Fig. 9 also includes correlations for a plane surface nickel electrode with [24] or without [28] turbulence promoters. Coefficients α, β, γ are given in Table 6; $\gamma = 0$ for a filter-press reactor and for the E3P reactor without pulsation.

From Table 6, mass transfer is higher for the E3P reactor (even without pulsation) than for a filter-press reactor. This may be explained by the flow-through configuration used in our experiments. Moreover, the real active surface area of the foam is not exactly known.

Under low pulsation conditions (low amplitude and frequency), mass transfer is enhanced at low Reynolds number relative to the hydrodynamic state without pulsation. Furthermore, when Reynolds number is higher than 200, pulsation seems to be inefficient. In contrast, under high pulsation (high amplitude and frequency), mass transfer is significantly increased

Table 6. Values of the coefficients of the correlations expressed as Sh against Re and data of the experimental conditions

Reference	*Electrode*	*Sc*	$10^{10}D$ /m^2 s^{-1}	*Re range*	$Sh = \alpha Sc^{-1/3}Re^{\beta}Sr^{\gamma}$
[23]	sheet of foam 60 p.p.i.	1570	6.4	24–280	$\alpha = 1.81$ $\beta = 0.39$ $\gamma = 0.00$
[24]	plane plate + turbulence promoter	1320	6.7	300–2200	$\alpha = 0.77$ $\beta = 0.57$ $\gamma = 0.00$
[24]	plane plate + sheet of foam 60 p.p.i.	1320	6.7	300–2300	$\alpha = 0.32$ $\beta = 0.61$ $\gamma = 0.00$
[28]	plane plate	1562	6.2	200–1000	$\alpha = 0.22$ $\beta = 0.71$ $\gamma = 0.00$
Present work	sheet of foam 60 p.p.i.†	989	10.4	30–250	$\alpha = 7.08$ $\beta = 0.36$ $\gamma = 0.00$
Present work	sheet of foam 60 p.p.i.‡	989	10.4	30–250	$\alpha = 2.77$ $\beta = 0.54$ $\gamma = 0.32$
Present work	sheet of foam 60 p.p.i.§	989	10.4	30–250	$\alpha = 2.77$ $\beta = 0.54$ $\gamma = 0.32$

* p.p.i.: pores per inch.
† Mass transfer without pulsation.
‡ Mass transfer with pulsation: $a = 0.2 \times 10^{-2}$ m and $f = 0.2$ Hz.
§ Mass transfer with pulsation: $a = 1.0 \times 10^{-2}$ m and $f = 1.0$ Hz.

and the Sherwood number is nearly tripled. The effectiveness of pulsation is constant over the whole studied range of Reynolds number.

4. Conclusion

The study of mass transfer at nickel foam electrodes under pulsed flow conditions shows that pulsation increases mass transfer coefficients, especially in the case of the low flow rates often required to achieve reasonable residence times. Nickel from MN100 gives the best mass transfer coefficients.

For materials such as nickel foam and expanded metals, amplitude and frequency of pulsation have the same influence on mass transfer, in contrast to what is observed when using fixed beds of spheres or particles [2].

The Sherwood number obtained for the mass transfer at a nickel foam electrode in a pulsed reactor is dramatically enhanced by the pulsation and is efficient over a large Re range, especially as the value of the instantaneous velocity $a\omega$ is high compared with U_0. However, the results show that the mass transfer can be limited under a high pulsation parameter. Then a compromise has to be found in order to set the best mass transfer conditions.

Controlling mass transfer conditions at nickel foam electrodes is critical to the control of the chemical selectivity of electroorganic reactions currently being investigated.

Acknowledgements

The authors thank the 'Department of Service Applications' de l'Electricité de France for financial support.

References

[1] A. Ratel, Thèse de Doctorat I.N.P.T., Toulouse (1987).
[2] A. Ratel, P. Duverneuil and G. Lacoste, *J. Appl. Electrochem.* **18** (1988) 394.
[3] A. Ratel and G. Lacoste, *ibid.* **12** (1982) 267.
[4] C. Molina, Thèse de Doctorat I.N.P.T., Toulouse (1991).
[5] J. Rodrigues de Souza, Thèse de Doctorat I.N.P.T., Toulouse (1993).
[6] S. Pouzet, N. Le Bolay and A. Ricard, *Synth. Met.* **55–57** (1993) 1495.
[7] *Idem, Electrochim. Acta* **38** (1993) 217.
[8] N. Le Bolay, J. F. Guilland and A. Ricard, *Chem. Eng. J.* **53** (1993) 137.
[9] N. Le Bolay, J. F. Guilland and A. Ricard, *Can. J. Chem. Eng.* **72** (1994) 153.
[10] C. Belmant, Thèse de Doctorat I.N.P.T., Toulouse (1993).
[11] H. J. Schäfer, *Top. Curr. Chem.* **142** (1987) 101.
[12] H. Rüholl and H. J. Schäfer, *Synthesis* (1988) 54.
[13] H. J. Schäfer and R. Schneider, *Tetrahedron* **47** (1991) 715.
[14] P. M. Robertson, P. Berg, H. Reimann, K. Scleich and P. Seiler, *J. Electrochem. Soc.* **130** (1983) 591.
[15] S. Langlois and F. Coeuret, *J. Appl. Electrochem.* **19** (1989) 43.
[16] L. E. A. Berlouis and G. J. Hills, *J. Electroanal. Chem.* **180** (1984) 401.
[17] A. Montillet, J. Comiti and J. Legrand, *J. Mater. Sci.* **27** (1992) 4460.
[18] S. Langlois, J. O. Nanzer and F. Coeuret, *J. Appl. Electrochem.* **19** (1989) 736.
[19] A. Montillet, J. Comiti and J. Legrand, *ibid.* **23** (1993) 1045.

[20] S. Langlois and F. Coeuret, *ibid.* **20** (1990) 740.
[21] *Idem, ibid.* **20** (1990) 749.
[22] A. Montillet, J. Comiti and J. Legrand, *Chem. Eng. J.* **52** (1993) 63.
[23] S. Langlois and F. Coeuret, *J. Appl. Electrochem.* **19** (1989) 51.
[24] A. Montillet, J. Comiti and J. Legrand, *ibid.* **24** (1994) 384.
[25] P. Cognet, J. Berlan, G. Lacoste and J. M. Jud, Collection 'Récents progrès en génie des procédés' **27** (1993) 99.
[26] SORAPEC, 192 rue Carnot, 94129 Fontenay sous Bois, France.
[27] P. Cognet, Thèse de Doctorat I.N.P.T., Toulouse (1994).
[28] C. J. Brown, D. Pletcher, F. C. Walsh, J. K. Hammond and D. Robinson, *J. Appl. Electrochem.* **23** (1993) 82.